Low-temperature properties of a dipolar glass: A study of KBr$_{1-x}$(CN)$_x$ using dielectric echoes

M. C. Foote*

University of Illinois, Urbana, Illinois 61801

Brage Golding

AT&T Bell Laboratories, Murray Hill, New Jersey 07974
(Received 25 October 1990)

Dielectric echoes have been used to study the low-temperature dynamics of the model orientational glass KBr$_{1-x}$(CN)$_x$. The echoes were observed at 0.79 GHz at temperatures between 10 and 60 mK for five single crystals with $0.000\,34 \leq x \leq 0.70$. The following properties of the CN$^-$ tunneling centers were measured: relaxation times (T_1), dephasing times (T_2), electric-dipole moments, and densities of states. Relative dielectric constants were also measured from 10 mK to room temperature. The results suggest that the nature of the tunneling centers, as characterized by their electric and elastic dipole moments, does not change significantly over the concentration range studied, but that the distribution in relaxation rates changes dramatically. We interpret this result in terms of variations in the symmetry of the double-well potentials characterizing these excitations.

I. INTRODUCTION

Low-energy tunneling excitations in solids display a variety of behavior at low temperature ($T < 1$ K). Identical dilute dopants in a crystalline solid typically possess a sharply peaked density of states and a single relaxation rate. In contrast, tunneling centers in glasses have broad distributions in energy and a range of relaxation rates due to their disordered environment. As a result, these two classes of materials exhibit strikingly different behavior at low temperature. In one widely studied material, KBr$_{1-x}$(CN)$_x$, the cyanide tunneling centers behave as noninteracting impurities in a crystal for low x, but as "glassy" excitations for x near 0.50 due to strong CN-CN interactions. In order to shed light on the development of these glassy properties as the cyanide concentration increases, we have studied KBr$_{1-x}$(CN)$_x$ for cyanide concentrations spanning this range of behavior. Dielectric echoes as well as dielectric susceptibility measurements were used to probe the low-energy excitations present in these materials in order to measure their electric-dipole moments, coupling strengths to strain, densities of states, and dephasing rates T_2^{-1}. We find that the coupling strength of the CN excitations to both electric and elastic fields varies little over the CN concentration range studied. An anomaly appears, however, in the scaling of T_2^{-1} with density of states, suggesting that the distribution of relaxation rates changes greatly with concentration. This result is interpreted in terms of variations in the tunneling-state symmetry distribution. In particular, we argue that for low x, the potential wells characterizing these excitations tend to be more symmetric than for high CN concentration. In addition, surprisingly long three-pulse echo decay times seen in the $x = 0.000\,34$ sample suggest the presence of a phonon bottleneck in this sample.

KBr$_{1-x}$(CN)$_x$ has a structure similar to sodium chloride, with bromine atoms and cyanide molecules randomly distributed among the sites of one of two sublattices. At room temperature this lattice is cubic, but various distorted phases are present at lower temperature.[1] Since KBr and KCN have nearly the same lattice constants, mixtures can form having any x value from 0 to 1. The cyanide molecules, although fixed in position, have some rotational freedom. Because of the random CN site distribution and strong elastic CN-CN interactions, the cyanide molecules, at $x \geq 0.01$, are affected by a range of potentials hindering their orientational motion. This distribution in reorientation potentials produces "glassy" low-temperature behavior for $x \sim 0.50$.

A qualitative phase diagram[1-3] for KBr$_{1-x}$(CN)$_x$ is shown in Fig. 1. The CN ions can rotate unhindered at high temperature, but the axis directions tend to freeze at lower temperatures due to strong elastic CN-CN interactions. This effect forms a ferroelastic phase with the CN axes aligned along $\langle 111 \rangle$ directions for $x > 0.57$, and an orientational glass for lower cyanide concentrations. Although with decreasing temperature the axes freeze, 180° reorientations can still occur until they are frozen at a somewhat lower temperature by electric-dipole interactions. For $x \geq 0.95$, an antiferroelectric phase is formed at low enough temperature, but over most of the concentration range the dipoles freeze randomly along their previously frozen axes, forming a dipolar glass. This picture of the CN freezing is somewhat controversial, and an alternate theory has been proposed to explain some possibly contradictory data.[4]

An isolated cyanide molecule in KBr tends to orient along one of the eight $\langle 111 \rangle$ directions,[5,6] resulting in eigenstates with four equally split energy levels[7] having degeneracies 1-3-3-1. Infrared spectroscopy[8] shows the energy splitting to be about 1.25 K. The narrow distribution in energy splittings of dilute CN doped into KBr results in a peak in the specific heat[9,10] and a dip in the
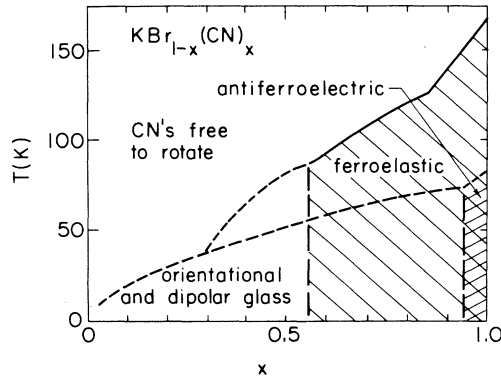
FIG. 1. Phase diagram for $KBr_{1-x}(CN)_x$ (Refs. 1–3). As the temperature is lowered, two "freezing" transitions occur, the first due to elastic and the second due to electric interactions. Dashed lines represent frequency-dependent transitions.

thermal conductivity[11,12] near 1 K. With increasing cyanide concentration these sharp features gradually broaden as interactions between CN molecules produce a distribution in energy splittings. For cyanide concentrations of 0.01 or greater, the specific heat exhibits a nearly linear temperature dependence[13,12] below 1 K, indicating a fairly constant density of states in the energy range 0.1 to 1 K. Although at $x=0.01$ this linear term is more than two orders of magnitude larger than the linear specific heat seen in glasses, the magnitude decreases to that of a glass as x approaches 0.50. The decreased density of states occurs because many of the CN excitations are frozen by their strong interactions with neighboring cyanide molecules.

Although long-time specific-heat measurements show a constant density of states like that of a glass for $x \geq 0.01$, time-dependent specific-heat measurements indicate that the distribution of relaxation times differs from a glass below $x=0.25$. From the distribution in relaxation times postulated for glasses,[14] a time-dependent specific heat varying as $\ln t$ is predicted, and, in fact has been observed[15] in amorphous SiO_2. $KBr_{1-x}(CN)_x$ samples with $x=0.01$ to 0.05, however, measured on a time scale of 50 ms to 5 s, showed a nonlogarithmic time dependence.[12,16] For cyanide concentrations in the range $0.25 \leq x \leq 0.70$, a specific heat varying logarithmically in time has been observed,[12] indicating that the distribution of relaxation times as well as the density of states is like that of a glass in this concentration range.

At $x=0.50$, $KBr_{1-x}(CN)_x$ is almost indistinguishable from a glass in its low-temperature properties. Its specific heat depends linearly on temperature[13,12] and as the logarithm of time;[12] its thermal conductivity varies as T^2 below 1 K and exhibits a plateau near 10 K.[13,12] In both cases the magnitudes are similar to those seen in glasses. Additionally, $KBr_{0.50}(CN)_{0.50}$ has a frequency-dependent minimum in its dielectric constant[13] below 1 K and a corresponding maximum in its sound velocity,[17] both features typical of glassy solids.

II. THEORY

A. Tunneling model

It will be convenient to discuss many of the results of this study in terms of the tunneling model for glasses, proposed by Anderson, Halperin, and Varma,[18] and by Phillips.[19] This model explains the sub-Kelvin excitations in glasses by a set of unspecified tunneling entities residing in double-well potentials. Each tunneling system is described by two parameters: (1) the asymmetry energy, or difference between the two potential energy minima, Δ, and (2) the tunnel splitting Δ_0, which is the Hamiltonian matrix overlap element between isolated harmonic-oscillator wave functions located in the two wells, and depends on the barrier height approximately as $\exp(-aV^{1/2})$. Glasses have broad distributions in Δ and Δ_0. The two lowest-energy eigenstates of this system have an energy splitting $E = (\Delta^2 + \Delta_0^2)^{1/2}$. Higher-energy states are neglected.

Among those states with a given energy splitting E, there will be distributions in the parameters $|\Delta|$ and Δ_0 varying from 0 to E. Symmetric tunneling centers ($\Delta \approx 0$, $\Delta_0 \approx E$) have strong *resonant* coupling to perturbing fields, so a perturbation can easily cause transitions between the eigenstates. This coupling allows symmetric states to easily absorb or emit resonant phonons. These *quickly relaxing states* are the excitations seen in thermal-conductivity and short-time specific-heat measurements. Their density of states is denoted by $\bar{P}$ in the tunneling model. For asymmetric states ($\Delta \approx E$, $\Delta_0 \approx 0$), the perturbing field has *relaxational* coupling, causing a change in the energy splitting, but few transitions.

The population or spin-lattice relaxation rate due to one-phonon processes for a tunneling center is given by[14]

$$T_1^{-1} = \left[\sum_\alpha \frac{\gamma_\alpha^2}{v_\alpha^5} \right] \left[\frac{\Delta_0}{E} \right]^2 \frac{E^3}{2\pi\rho\hbar^4} \coth \left[\frac{E}{2kT} \right], \quad (1)$$

where α labels the phonon modes. In an anisotropic solid such as $KBr_{1-x}(CN)_x$, the sum also includes an average over crystalline directions. The quantity ρ denotes the density.

The tunneling model postulates a constant distribution in Δ and a distribution in Δ_0 that varies as $1/\Delta_0$. The joint distribution in E and T_1^{-1} is given by

$$P(E, T_1^{-1}) = \frac{\bar{P}}{2T_1^{-1} \left[1 - \dfrac{T_1^{-1}}{T_1^{-1}(\text{max})} \right]^{1/2}}, \quad (2)$$

where $T_1^{-1}(\text{max})$ represents the maximum relaxation rate at a given energy—that of the symmetric states. Figure 2 illustrates this distribution of relaxation rates.

Tunneling centers contribute to the low-temperature dielectric constant in two ways. The symmetric states contribute a "resonant" term, which is seen as a *decrease* in ϵ with increasing temperature below 1 K near 1 GHz. The asymmetric states produce an *increase* in ϵ with increasing temperature at $T > 1$ K in the 1-GHz range due to relaxation. A minimum in ϵ near 1 K marks the cross-
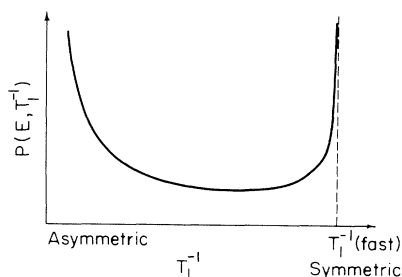
FIG. 2. The distribution of relaxation rates at a given energy in the tunneling model [Eq. (2)]. T_1^{-1}(fast) is the fastest relaxation rate at this energy.

over between these two competing effects. Below 1 K, the "resonant" term gives[20]

$$\Delta\epsilon/\epsilon = -\frac{2\,\bar{P}p_0^2}{3\epsilon_0\epsilon}\ln\left[\frac{T}{T_0}\right] , \qquad (3)$$

where T_0 denotes an arbitrary reference temperature. Below $T \approx hf/k$, ϵ is temperature independent.

B. Dielectric echoes

Golding and Graebner[21] first demonstrated the existence of echo phenomena in glasses, analogous to echoes in magnetic resonance, by using *elastic* excitation of the tunneling centers. In *dielectric*-echo experiments, developed by Golding et al.[22] and Bernard et al.,[23] a sequence of oscillating electric field pulses excites resonant tunneling states, producing coherent dephasing and rephasing of their wave functions. The echoes produced by this rephasing allow one to measure relaxation times of tunneling states, electric-dipole moments, densities of states, and matrix elements coupling states to elastic strain.

Three different pulse sequences were used in the present experiments:[24] the two-pulse sequence, the three-pulse inversion-recovery sequence, and the stimulated-echo sequence. In a two-pulse echo experiment, two pulses, separated by a time τ, produce an echo after an additional time τ. The decay of this echo amplitude as a function of 2τ measures the dephasing time T_2, governed by interactions between tunneling centers. The two-pulse echo amplitude before decay is given by[24]

$$A = B\bar{P}p\sin\left[\frac{\mathscr{E}pt_1}{\hbar}\right]\sin^2\left[\frac{\mathscr{E}pt_2}{2\hbar}\right] , \qquad (4)$$

where $\mathscr{E}$ is the electric field strength in the sample, p the component of electric-dipole moment along the field direction, and t_i is the pulse width of the ith pulse. The quantity B depends on the experimental conditions. For the case of $t_2 = 2t_1$, Eq. (4) reduces to

$$A = B\bar{P}p\sin^3\left[\frac{\mathscr{E}pt_1}{\hbar}\right] . \qquad (5)$$

This expression gives the shape of the "excitation curve." A peak occurs as a function of $\mathscr{E}$ at $\mathscr{E}pt_1/\hbar = \pi/2$, and

the dipole moment can be determined from the relation $p = (\pi/2)(\hbar/\,t_1\mathscr{E}_{\text{peak}})$. When there is a distribution in p, the quantity A must be integrated appropriately.

The first pulse of a three-pulse inversion-recovery experiment (Fig. 3) produces a π rotation, inverting the population of states. The population decay back to the ground state by interactions with phonons is monitored by applying a two-pulse echo sequence at a later time τ_{12}. If this two-pulse sequence immediately follows the inverting pulse [Fig. 3(a)], an inverted echo will be observed with a phase-sensitive detector. As τ_{12} is increased, the echo will recover to its original value [Fig. 3(b)] with the characteristic time T_1.

The stimulated-echo sequence consists of two $\pi/2$ pulses separated by a time τ_{12}, a third $\pi/2$ pulse at τ_{13}, and an echo after an additional time τ_{12}. The echo-amplitude decay as a function of τ_{12} and τ_{13} depends on both T_1 and T_2, and provides information on the role of spectral diffusion in the dephasing process.

C. Spectral diffusion

Spectral diffusion is a process by which excitation is transferred across an absorption band. The mechanism of this diffusive transfer that is believed to dominate in glasses[25] can be seen by dividing the tunneling centers into A states, those resonantly excited in an echo experiment, and the thermally active B states whose motion perturbs the A states. The A states are predominantly symmetric tunneling centers—those that can resonantly couple to the applied electric pulses. The B states also need some symmetric character so that thermal phonons may activate them, but they must also be somewhat asymmetric to couple to the A states, since this coupling is given by[25]

$$J_{ij} = \frac{C_{ij}}{r_{ij}^3}\left[\frac{\Delta_i}{E_i}\right]\left[\frac{\Delta_j}{E_j}\right] , \qquad (6)$$

where r_{ij} is the distance between tunneling centers i and j, and C_{ij} depends on the elastic- or electric-dipole moment of the two states. Thus, in a glass, the states believed to cause dephasing are typically more asymmetric
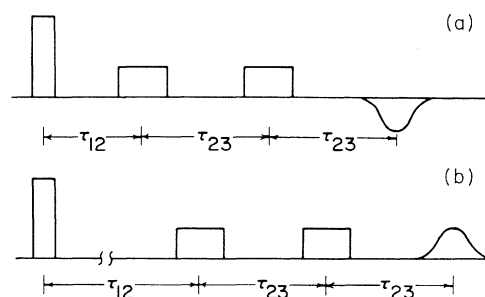

FIG. 3. Three-pulse inversion-recovery pulse sequence in two limits. (a) The two-pulse probing sequence is applied immediately after the inverting pulse, the echo is inverted. (b) The two-pulse probing sequence occurs at long time after the inverting pulse, the echo is upright and unaffected by inverting pulse.

than the states that are observed directly in the echo experiment.

III. EXPERIMENT

$KBr_{1-x}(CN)_x$ samples with $x = 0.03$, 0.20, 0.50, and 0.70 were obtained from the Crystal-Growth Laboratory at the University of Utah, and an $x = 0.000\,34$ CN sample was provided by S. Susman of Argonne National Laboratory. Quoted cyanide concentrations are believed accurate to about 15%. The $x = 0.03$, 0.20, and 0.50 samples are from the same crystals as those used in low-temperature specific-heat, thermal-conductivity, and dielectric permittivity measurements.[13,26] Pieces of the $x = 0.000\,34$ sample have been used in specific-heat[10] and neutron scattering measurements.[27] Time-dependent specific-heat measurements were performed on the $x = 0.01$ and 0.03 samples.[16] In addition, thermal expansion measurements have been made on the $x = 0.000\,34$ and 0.50 samples.[10] The major impurity in these crystals is believed to be $(CNO)^-$, which is present at a level of 0.1 parts per 10^9 in the $x = 0.000\,34$ sample,[27] and at 100–500 ppm in the other samples.[26]

Octagonal disks roughly 1 cm in diameter and 1.8 mm thick, and $\langle 100 \rangle$ oriented, were cut from the $KBr_{1-x}(CN)_x$ boules. Preparation of samples was carried out partly in a nitrogen-filled dry box and partly in air with a light coat of mineral oil covering the sample as a protection against moisture.

The apparatus used in this work was used in earlier echo studies.[28,29] Samples were placed in a copper microwave resonant cavity attached to the mixing chamber of a dilution refrigerator. Two copper loops coupled magnetically to the TEM mode of the cavity, and were attached to the room-temperature electronics via coaxial cables. The electric field was applied along a $\langle 100 \rangle$ direction. Loaded resonant frequencies of the cavities were about 790 MHz, and Q values were approximately 200.

Variations in the dielectric constant of the $KBr_{1-x}(CN)_x$ samples were measured by phase locking a voltage-controlled oscillator to the resonance and recording the oscillator frequency as a function of temperature.

Because the echo signals were very weak in some cases, they were averaged for as many as 10^5 sequences. The repetition rate was low enough that bulk heating of the samples was minimized. Estimated temperature uncertainties due to heating are indicated by error bars in the figures.

Pulse powers used were of an intensity about 1–4 dB below that required for maximum echo generation, minimizing distortion of the echo shapes resulting from inhomogeneous broadening and distributions in the electric-dipole moment. Pulse widths for two-pulse and stimulated echoes were generally 0.4 μs, although for determination of the echo excitation curves of Sec. IV B, two-pulse sequences of 0.3 and 0.6 μs duration were used. The three-pulse inversion-recovery experiments used a 0.3-μs inverting pulse and probing pulses of 0.7–1.0 μs. A narrower inverting pulse excited a broad spectral range

of tunneling centers. The probing two-pulse sequence observed a narrower band of states, so sampled only the center of the excited band where the states were substantially inverted.

IV. RESULTS AND DISCUSSION

A. Dielectric measurements

Figure 4 shows relative variations with temperature of the real part of the dielectric constant for the five $KBr_{1-x}(CN)_x$ samples. The high-temperature features seen in the $x = 0.03$–0.70 samples have been previously observed:[31,32] a positive $d\epsilon/dT$ near room temperature due to the ionic crystal lattice (labeled a on the $x = 0.03$ data in Fig. 4), a negative $d\epsilon/dT$ or shoulder near 50 K from paraelectric behavior of the CN ions (b in Fig. 4), and finally the electric-dipole freezing (c in Fig. 4). Figure 5 shows the $KBr_{1-x}(CN)_x$ dielectric data at low temperature on an expanded vertical scale. In the region $0.1 < T < 1$ K, all of the samples exhibit an approximately $\ln T$ resonant behavior typical of glassy solids (indicated by the dashed lines).

The shape of the $x = 0.000\,34$ $\Delta\epsilon/\epsilon$ versus T curve can be approximately explained by contributions from the KBr ionic lattice at high temperature and from ideal CN dopants in KBr at low temperature. The CN concentration is too low to exhibit substantial paraelectric behavior, and presumably the CN tunneling rate is high enough to prevent freezing from being observed, so features b and c described above are absent in these data. Figure 6 shows the $x = 0.000\,34$ data (solid line), as well as a curve representing the sum of the measured dielectric constant[33] of pure KBr (dashed line above 10 K) and
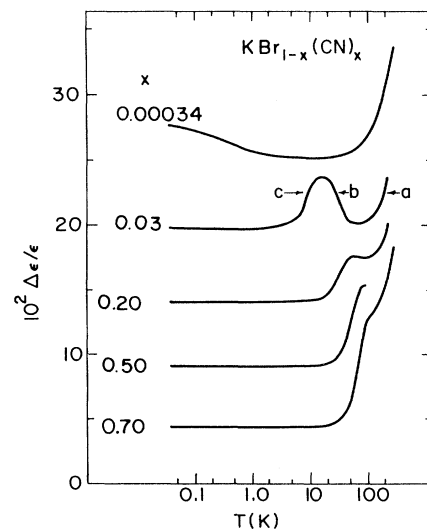

FIG. 4. Relative changes in the real part of the 0.79-GHz dielectric constant with temperature for the five $KBr_{1-x}(CN)_x$ samples. Data are offset vertically from each other for clarity. A smooth curve has been drawn through each set of > 100 data points. Scatter is $\Delta\epsilon/\epsilon \leq 10^{-3}$. Regions a, b, and c are discussed in the text. The actual data appear in Ref. 30.
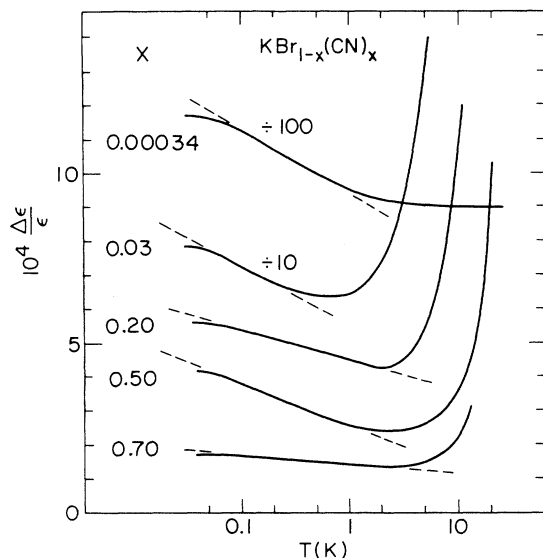
FIG. 5. Relative variations in the real part of the 0.79-GHz dielectric constant vs temperature for the five CN concentrations. The data are offset from each other vertically for clarity. Note that the $x=0.03$ data are reduced by a factor of 10 and the $x=0.00034$ data by a factor of 100. A smooth curve has been drawn through each set of >100 data points. Scatter is $\Delta\epsilon/\epsilon \sim 4\times10^{-5}$. Dashed lines represent slopes of the resonant $\ln T$ region at $0.1<T<1$ K. The actual data appear in Ref. 30.

FIG. 6. Changes in the real part of the 0.79-GHz dielectric constant for $x=0.00034$ $KBr_{1-x}(CN)_x$. Solid line: measured values; dashed line: "calculated" values (Ref. 30), as described in the text. The two curves are offset vertically from each other for clarity.

the calculated dielectric constant for a 0.00034 concentration of ideal CN tunneling centers in KBr (Ref. 30) [dashed line below 10 K, this calculation assumes $E=1.25$ K (Ref. 8), $p=0.5$ D (Ref. 34), and $\epsilon=4.7$ (Ref. 31)]. The calculated total change in ϵ between 0.1 and 10 K agrees well with measurement, indicating that the majority of cyanide impurities participate in this tunneling process. It is significant that the measured dielectric constant for the $x=0.00034$ sample flattens off at a lower temperature than the calculated value (about 50 mK as compared to 500 mK). The distribution in energy splittings of CN excitations must therefore be broad enough to include values of energy much lower than the 1.25 K of an unperturbed CN site in KBr. This conclusion is consistent with results from specific-heat measurements[10] on a piece of the same crystal. The spread in energy splittings has been tentatively ascribed[10] to weak interactions between CN molecules. Since dielectric echoes
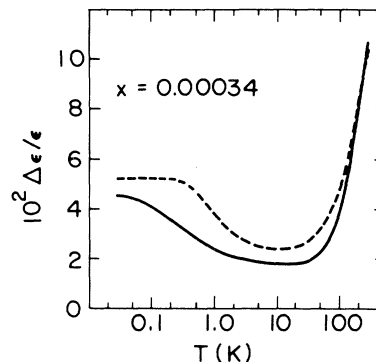
were observed in this sample at 0.79 GHz (corresponding to an energy splitting of about 40 mK), the existence of a spread in energy splittings which allows 40-mK states is also necessary to explain the echo results.

From the slope of the low-temperature dielectric constants in the range $0.1<T<1$ K (Fig. 5), one can obtain densities of states for symmetric tunneling centers in $KBr_{1-x}(CN)_x$ using Eq. (3), with $\epsilon=4.7$ (Ref. 31) and $p=0.5$ D (Ref. 34). Since the roughly linear specific heat in all but the $x=0.00034$ sample shows that there are broad distributions in tunneling parameters, the use of this formula developed for glasses seems justified. The resulting $\bar{P}$ values are given in Table I, and can be seen to be in reasonable agreement with values derived from other experiments.

B. Echo excitation measurements

Figure 7 shows the two-pulse echo amplitude as a function of applied electric field strength for the five samples studied. An intriguing result is that the maxima occur at approximately the same value of electric field ($\pm 20\%$, which is within the experimental uncertainty), showing that the typical value of electric-dipole moment is nearly independent of cyanide concentration [Eq. (5)]. The dipole moment is therefore about 0.5 D for all samples, as

TABLE I. Comparison of $\bar{P}$ derived from dielectric (this work), time-dependent specific-heat (Ref. 12), and sound-velocity measurements (Ref. 35). Note that $\bar{P}$ from the $x=0.20$ dielectric measurements is compared to $\bar{P}$ from specific-heat and velocity measurements on $x=0.25$ samples.

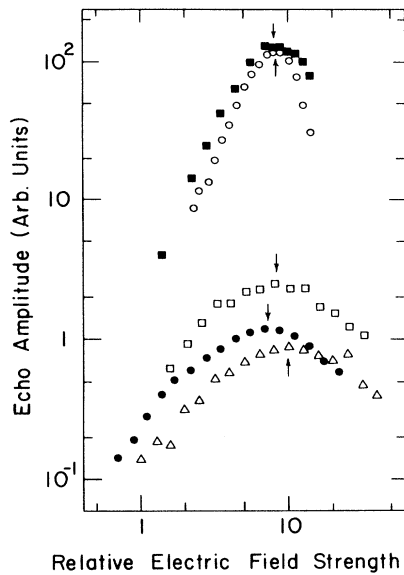| x	$\bar{P}$ from $\Delta\epsilon/\epsilon$ $(10^{45}\ J^{-1}m^{-3})$	$\bar{P}$ from $C(t)$ $(10^{45}\ J^{-1}m^{-3})$	$\bar{P}$ from $\Delta v/v$ $(10^{45}\ J^{-1}m^{-3})$
0.00034	170		
0.03	16		
0.20	0.83	$(x=0.25)$ 4.0	$(x=0.25)$ 3.1
0.50	1.2	0.9	1.4
0.70	0.20	0.27	

FIG. 7. Two-pulse echo amplitude as a function of electric field strength near 10 mK for $x=0.00034$ (■), $x=0.03$ (○), $x=0.20$ (□), $x=0.50$ (●), and $x=0.70$ (△). Units are arbitrary, but are the same for all samples. The arrows indicate approximate positions of the peaks.

it is for an isolated CN ion in KBr.[34]

A qualitative picture of the distribution in dipole moments can be obtained from the shapes of the excitation curves. The curves for the 0.000 34 and $x=0.03$ samples are sharply peaked, while the $x=0.20$, 0.50, and 0.70 excitation curves are much broader. The normalized $x=0.03$ and 0.50 echo amplitudes are plotted together in Fig. 8, with an excitation curve calculated for a single value of dipole moment [dashed line, Eq. (5)]. The $x=0.03$ peak is fitted well with a single value of dipole moment, but the $x=0.50$ sample requires a distribution in p to explain the broadened maximum.

Two possible sources of broadening in excitation

curves are (1) an angular distribution of dipole orientations and (2) a distribution of dipole moments due to the distributions postulated in the tunneling model. These effects have been shown[36,37,30] not to alter the shape of the low-power excitation curve significantly from that of a single dipole moment, so it is not clear whether the $x=0.00034$ and 0.03 data represent a single value of dipole moment or a distribution in p due to these effects.

The two distributions of electric dipoles discussed above cannot, however, account for the broad excitation curves of the $x=0.20$, 0.50, and 0.70 samples. Because of the effects of inhomogeneous broadening on the echo shape, it is difficult to interpret the shape of the excitation curve for powers larger than the peak value. The broadening at low power in the high-concentration samples, however, clearly indicates the presence of excitations with larger dipole moments than that value corresponding to the peak. The distribution in p for $KBr_{0.50}(CN)_{0.50}$ must extend to values of p at least one order of magnitude larger than 0.5 D, since the broadening is present at an electric field which is a factor of 10 below the peak value. These large dipole moments may be due to impurities such as $(CNO)^-$, which should be present in lower concentrations in the $x=0.00034$ and 0.03 samples. A more interesting possibility is that some fraction of the tunneling centers in the high-concentration samples may be clusters of CN molecules which, as a group, have a larger dipole moment than a single CN tunneling center.

A study of rotary echoes[38] in $x=0.03$ and 0.20 $KBr_{1-x}(CN)_x$ also shows a narrow p distribution in $KBr_{0.97}(CN)_{0.03}$ and a broad distribution in $KBr_{0.80}(CN)_{0.20}$. However, unlike our results, the p distribution in $KBr_{0.80}(CN)_{0.20}$ could be explained approximately by the tunneling model distributions.

C. Measurement of T_2

Decays of two-pulse echoes for the $x=0.50$ sample from 10 to 60 mK are shown in Fig. 9. The nonexponen-
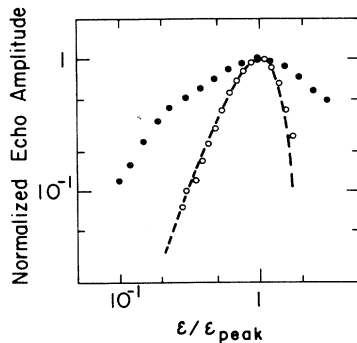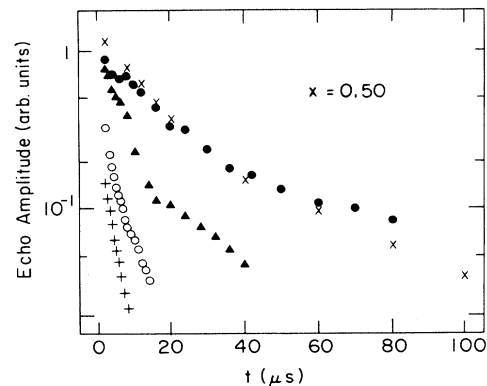

FIG. 8. The $x=0.03$ (○) and 0.50 (●) excitation curves graphed in normalized units so that the peaks occur at the same electric field and are the same height. The dashed line is a calculated curve, assuming a single value of dipole moment [Eq. (5)].

FIG. 9. Two-pulse echo decays for $KBr_{0.50}(CN)_{0.50}$ of temperatures of 10 mK (●), 13 mK (×), 20 mK (▲), 40 mK (○), and 60 mK (+). The fact that the initial echo amplitude at 13 mK is larger than at 10 mK is probably an experimental artifact due to slightly different detector sensitivities.

tial nature of the decays made it impossible to obtain a unique decay time from each decay, so T_2 was defined as the initial echo-amplitude decay time. T_2 versus temperature for the five samples is plotted in Fig. 10, along with values from intrinsic tunneling centers and OH-impurity centers in SiO_2 glass for comparison. The value of $T_2 = 4$ μs at 30 mK for $KBr_{0.97}(CN)_{0.03}$ from rotary echoes[38] is in the same range as these data.

The nonexponential nature of the decays differs from predictions of exponential decay shapes in glassy systems which have dipolar interactions between tunneling centers.[39] Exponential decays have been observed for both the "intrinsic" tunneling centers and for OH-impurity centers in SiO_2 glass[40] (Fig. 11), as well as in Nd^{3+}-doped SiO_2 fibers.[41] Subexponential decays have, however, been seen in As_2S_3 (Ref. 28) and Na β-alumina,[37] both of which are glassy systems, and in polyethylene,[42] in which some tunneling centers may reside in a crystalline environment.[43]

A possible reason for the subexponential two-pulse echo decays in $KBr_{1-x}(CN)_x$ is that the interaction between tunneling centers may not be dipolar. For dipolar systems the interaction strength varies as $1/r^3$, but perhaps in $KBr_{1-x}(CN)_x$ it varies as $1/r^4$ or $1/r^5$. For a system of tunneling centers having tunneling model distributions and $1/r^n$ interactions, the two-pulse echo decay shape is predicted to be[39]

$$A = A_0 \exp(-Cn_0 T t^{3/n}) , \qquad (7)$$

where C depends on the strength of the $1/r^n$ coupling between states and n_0 is the density of states of B
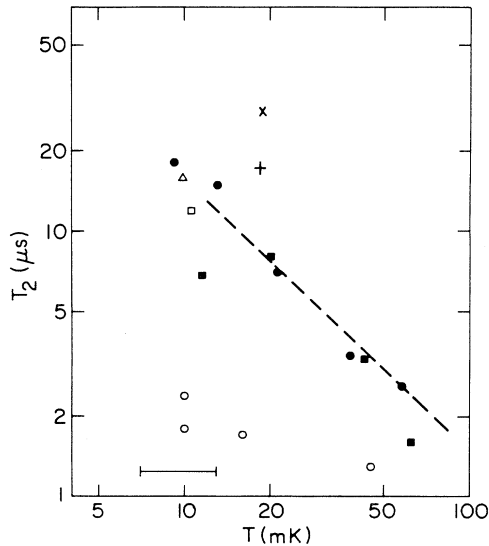

FIG. 11. Two-pulse echo decays for "intrinsic" ($\bullet$) and OH-impurity ($\circ$) tunneling centers in SiO_2 glass (Ref. 40). Strict exponential behavior is observed. The units on the vertical scale are arbitrary.

states. We might postulate that the interactions in $KBr_{1-x}(CN)_x$ vary as $1/r^5$, and attempt to fit the observed decays to a function of the form

$$A = A_0 \exp(-\alpha t^{3/5}) . \qquad (8)$$

An example of such a fit for the $x = 0.50$ sample at 13 mK is shown in Fig. 12. The $\exp(-\alpha t^{3/5})$ decay [Fig. 12(b)] clearly fits the data better than the exponential [Fig.

FIG. 10. Two-pulse echo decay times as a function of temperature for $x = 0.00034$ ($\blacksquare$), $x = 0.03$ ($\circ$), $x = 0.20$ ($\square$), $x = 0.50$ ($\bullet$), and $x = 0.70$ ($\triangle$). Values of T_2 for intrinsic ($+$) and OH-related ($\times$) tunneling centers in SiO_2 glass at 0.72 GHz are also shown for comparison (Ref. 22). The dashed line indicates a T^{-1} temperature dependence. The uncertainty in temperature of the lowest-temperature points is indicated by the error bar at the bottom of the figure. Higher-temperature points have much smaller uncertainties in temperature.
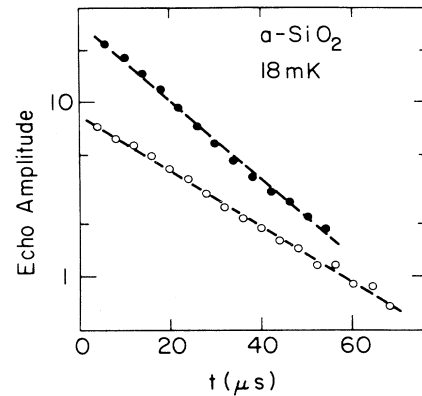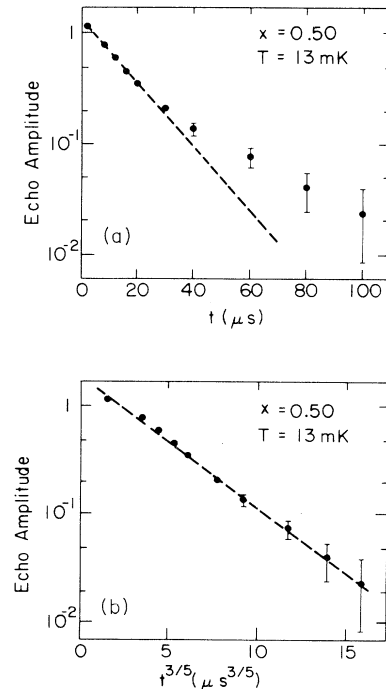

FIG. 12. A two-pulse echo decay for $KBr_{0.50}C(N)_{0.50}$ at 13 mK (a) plotted on a log-linear scale; (b) plotted as $\log_{10}$(amplitude) vs $t^{3/5}$. The time t denotes the time interval between the first pulse and the echo ($t = 2\tau$).

12(a)]. The other decay curves from the $x=0.03$, 0.20, 0.50, and 0.70 samples yielded similar results, although for the fastest decays it was impossible to differentiate between the two decay forms. Thus the decay shapes observed were *consistent* with a $1/r^5$ interaction.

The temperature dependence of dephasing times in glasses has not been explained well by theory. For a glass, one expects the dephasing rate to vary roughly linearly with temperature [Eq. (7)]. The observed behavior, however, ranges from $T^{0.65}$ in Na β-alumina[37] to T^2 for the intrinsic states in SiO_2 glass.[44,45] A dephasing rate varying linearly with temperature is indicated by the dashed line in Fig. 10, and can be seen to be consistent with the $x=0.50$ data. The two-pulse decay time for the $x=0.03$ sample, however, has a much weaker temperature dependence.

D. Inverse-recovery (T_1) measurements

1. T_1 results for the $x=0.03-0.70$ samples

The three-pulse inversion-recovery experiment was used to measure spin-lattice relaxation times (T_1). Figure 13 illustrates the recovery of echo amplitude after inversion for the $x=0.03$ and 0.50 samples at 10 mK. Inversion of the echoes was only achieved for the $x=0.00034$ and 0.03 samples; with the 0.20, 0.50, and 0.70 samples the echo amplitude could only be reduced to zero. This resistance to echo inversion in the high-concentration samples might be caused by the broad distribution in dipole moments that we have found to be present in these samples.

Values of T_1 obtained from the initial decays for the $x=0.03$, 0.20, 0.50, and 0.70 $KBr_{1-x}(CN)_x$ samples are shown in Fig. 14. The solid line indicates the $\tanh(E/2kT)$ behavior expected for one-phonon process-

es, and has been adjusted in amplitude to match the measured T_1 of the $x=0.50$ sample at 10 mK. The value of $T_1=20\,\mu s$ at 30 mK and 800 MHz in $KBr_{0.97}(CN)_{0.03}$ obtained from rotary echoes[38] is in the same range as our data.

The coupling strength γ between tunneling centers and phonons can be calculated from measured T_1 values using Eq. (1). Initial decay rates correspond to states with $\Delta_0=E$. Equation (1) can be solved approximately for γ, with the result

$$\gamma = \left[\frac{v_D^5 \rho h}{3(2\pi f)^3 T_1} \right]^{1/2} , \qquad (9)$$

where T_1 is the measured value at 10 mK [where $\coth(E/2kT)\approx 1$], and v_D is the Debye velocity tabulated in Ref. 12. We estimate[30] that the error involved in using this Debye velocity rather than the correct value obtained by averaging $1/v^5$ over all crystalline directions is less than a factor of 2. Values of γ calculated by this method, along with the numbers used in their calculation, are tabulated in Table II.

The coupling strengths obtained from echo experiments can be compared to values derived from time-dependent specific-heat experiments combined with thermal-conductivity measurements[12] (Table II). Good agreement is seen between the two experiments for the $x=0.50$ and 0.20–0.25 samples. The lack of agreement for the $x=0.70$ sample probably indicates that the low thermal conductivity in this sample is not solely to phonon scattering from tunneling centers. It is likely that other scattering mechanisms are present such as scattering from the ferroelastic domain walls. A more complete discussion of this point is provided in Ref. 12. In any case, the echo experiment provides a more direct means of measuring the coupling of tunneling centers to pho-
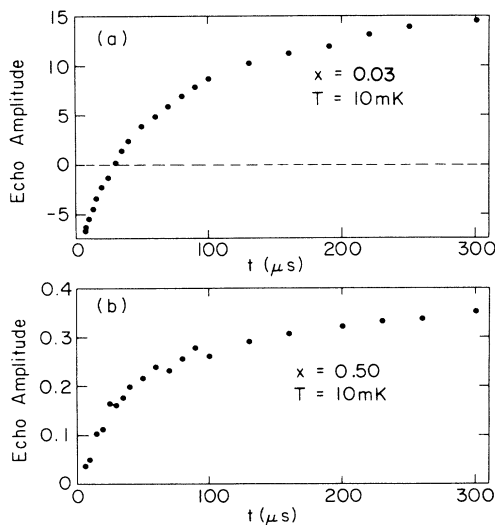

FIG. 13. Recovery of echo amplitude after inversion or saturation for the $x=0.03$ and 0.50 $KBr_{1-x}(CN)_x$ samples. The time scale on the horizontal axis represents the time between the initial inverting pulse and the echo.
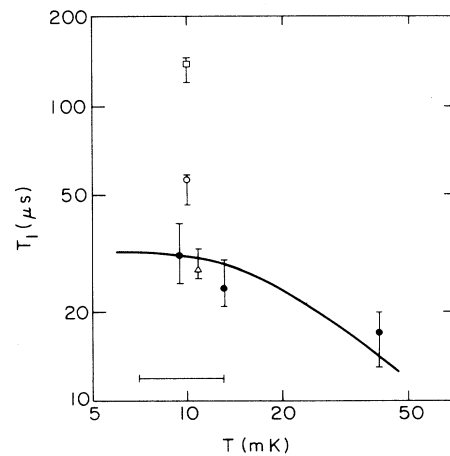

FIG. 14. Spin-lattice relaxation times (T_1) as a function of temperature for $x=0.03$ ($\bigcirc$), $x=0.20$ ($\square$), $x=0.50$ ($\bullet$), and $x=0.70$ ($\triangle$). The solid line represents the $\tanh(E/2kT)$ behavior expected for one-phonon processes. Temperature uncertainty for the lowest-temperature points is indicated by the error bar at the bottom of the figure.

TABLE II. The second through fifth columns are values used in the calculation of γ. The density ρ and the Debye velocity v_D were obtained from Ref. 12, and T_1 is from results of three-pulse inversion-recovery experiments near 10 mK. Calculated values of γ are given in the sixth column, and compared to values obtained from time-dependent specific-heat combined with thermal-conductivity (Ref. 12) and sound-velocity measurements (Ref. 35). Note that the calculated $\gamma = 0.20$ sample is compared to thermal and acoustic measurements on $x = 0.25$ samples.

x	ρ (10^3 kg/m^3)	v_D (10^3 m/s)	f (MHz)	T_1 (μs)	γ, this work (eV)	γ from $C(t)$ and κ (eV)	γ from $\Delta v/v$ (eV)
0.000 34	2.82	1.88	792	180	0.15		
0.03	2.78	1.72	785	56	0.23		
0.20	2.56	1.55	794	137	0.11	($x = 0.25$) 0.12	($x = 0.25$) 0.16
0.50	2.18	1.48	798	31	0.18	0.18	0.15
0.70	1.95	1.63	800	28	0.23	0.48	

nons than the thermal measurements. Values of γ for $x = 0.25$ and 0.50 KBr$_{1-x}$(CN)$_x$ also compare well with those obtained from measurements of sound velocity and acoustic attenuation[35] at $T < 1$ K. The various values of γ are similar to the value of 0.15 eV for an isolated CN molecule in KBr, which was deduced[6,12] from infrared spectroscopy.

2. Inversion-recovery results
for the $x = 0.000\,34$ CN sample

The three-pulse echo decays from the $x = 0.000\,34$ CN sample displayed anomalously long relaxation times. At $T \leq 10$ mK one expects $T_1 \approx 200$ μs from the value $\gamma = 0.15$ eV for the coupling strength between an isolated CN in KBr and the $\langle 100 \rangle$ transverse phonons,[6,12] however, the recovery times seen in the three-pulse inversion-recovery experiment are orders of magnitude longer than this estimated value. Figure 15 shows these decays at four temperatures, plotted as a function of $\ln t$ in order to include all data on the same graph. The dashed curve represents an exponential decay with $T_1 = 200$ μs, assuming that the echo is initially inverted 50%. At 10 mK, the system is still relaxing after 0.1 s—

more than two orders of magnitude longer than expected. Extremely long relaxation times such as these were not seen in the other KBr$_{1-x}$(CN)$_x$ samples. The data of Fig. 15 at 10 and 20 mK are plotted in Fig. 16 at both (a) short times and (b) long times as absolute differences between the echo amplitude at a given time and the completely recovered amplitude. The time scales on the two plots differ by a factor of 1000, and it is clear that the decays are not exponential on any time scale within the
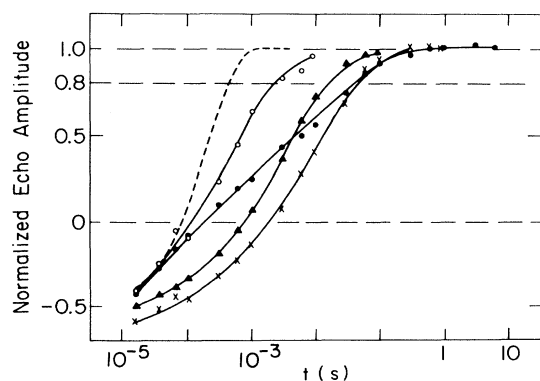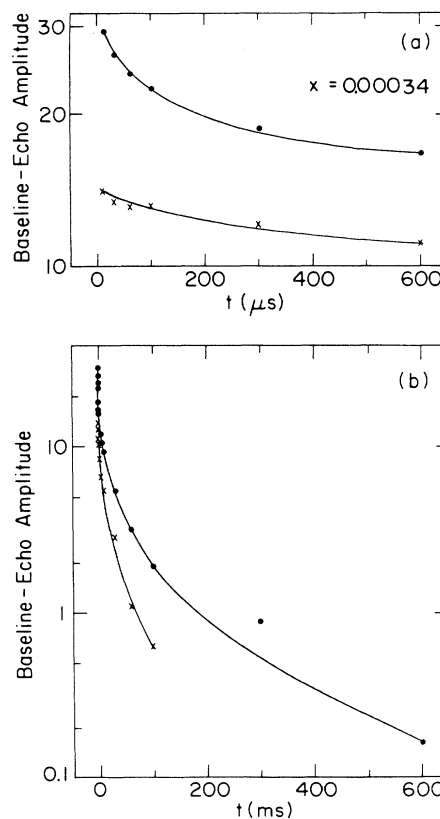

FIG. 15. Recovery of echo amplitude after inversion from the three-pulse inversion-recovery experiment for the $x = 0.000\,34$ sample at 10 mK ($\bullet$), 20 mK ($\times$), 38 mK ($\blacktriangle$), and 68 mK ($\circ$). The dashed curve represents the decay expected if all states have $T_1 = 200$ μs and the echo is initially 50% inverted. Solid lines through data sets are guides to the eye.

FIG. 16. Data of Fig. 15 for 10 ($\bullet$) and 20 mK ($\times$) plotted as the difference between the echo amplitude and the amplitude of a completely recovered echo. (a) Initial decay at short time. (b) Long-time decay. Solid lines are guides to the eye.

range of measurement. Initially, the 10-mK curve decays with a time constant of about 180 μs, consistent with the expected behavior. At the longest times, however, the instantaneous decay time is 200 ms.

The long decays of Figs. 15 and 16 might be explained by the presence of a phonon bottleneck, which occurs when the excited tunneling states heat the resonant lattice modes far above equilibrium, and these phonons are slow to equilibrate with their environment. In the presence of a phonon bottleneck, the decay time close to thermal equilibrium is given by[46]

$$\tau_{BN} = \frac{N_{TC}\tau_{ph}}{N_{ph}} \tanh^2(E/2kT) , \tag{10}$$

where N_{TC} and N_{ph} are the densities of states for tunneling centers and phonons, respectively. The quantity τ_{ph}, which is the characteristic equilibration time for the phonons with their environment, is estimated to be about 200 ms from a random-walk calculation[30] involving interactions with resonant tunneling centers and eventual equilibration at the surfaces of the crystal. One therefore obtains $\tau_{BN} \approx A \tanh^2(E/2kT)$, with $A = 20$ min. The recovery times for 80% recovered echoes in $x = 0.00034$ $KBr_{1-x}(CN)_x$ (close to thermal equilibrium, amplitude of 0.8 in Fig. 15) are plotted as a function of temperature in Fig. 17. These times closely follow the curve $\tau = (60$ ms$)\tanh^2(E/2kT)$, which has the correct temperature dependence for a bottleneck but a smaller prefactor, perhaps because the phonons actually equilibrate within the crystal before reaching the boundary.

Often when conditions favor a bottleneck, and a system of spins is inverted, the initial decay is actually much quicker than T_1, a phenomenon termed a "phonon avalanche." As the inverted population begins to decay, the phonon modes heat up, accelerating the spin decay towards saturation. The initial decay times, shown in Fig. 18, do not indicate a strong avalanche, but the fact
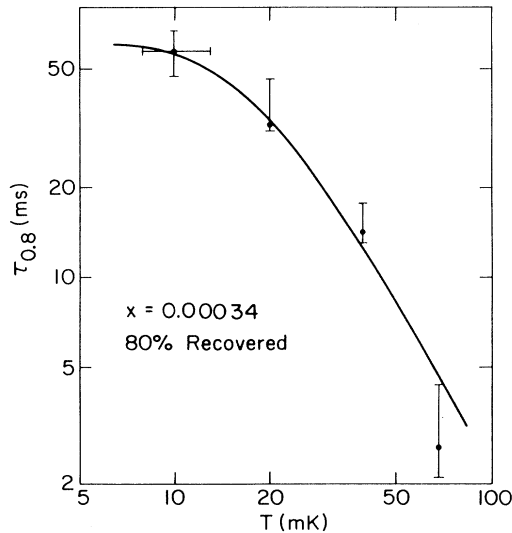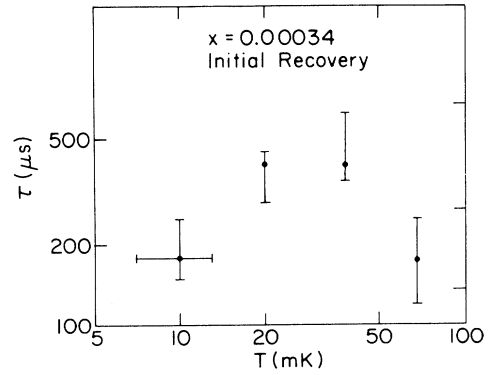

FIG. 18. Initial decay times for the population recoveries of Fig. 15.

that the 10-mK initial decay is faster than the initial decay at 20 mK is suggestive of an avalanche.

In short, results from three-pulse inversion-recovery experiments on the $x = 0.00034$ CN sample are not completely understood, however, the phonon-bottleneck picture seems to be a plausible explanation for most of the data.

E. Stimulated-echo measurements

Evidence for the presence of spectral diffusion has been seen in glasses[29,44] by observing the decay of the stimulated echo as a function of total time between the first pulse and echo $(\tau_{13} + \tau_{12})$ for several different values of τ_{12}. If spectral diffusion is present, the decay rate increases with increasing τ_{12}, although a good quantitative comparison between theory and experiment has not been obtained for this effect in glasses. Figure 19 shows the decay of the stimulated echo in $KBr_{0.50}(CN)_{0.50}$ as a function of total decay time $\tau_{13} + \tau_{12}$ for three different values of τ_{12}. The variation of decay rate at short τ_{12} clearly indicates the presence of spectral diffusion.

Stimulated-echo experiments are often used to measure the spin-lattice relaxation time T_1, since a decay time measured with this technique will be a lower bound for
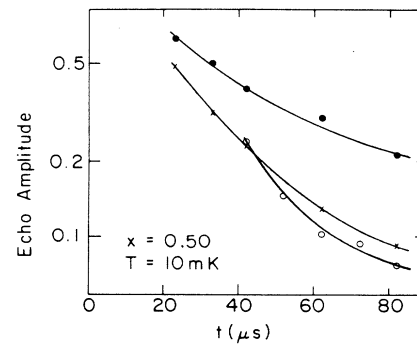

FIG. 17. Echo-amplitude recovery time for the $x = 0.00034$ sample when echo has recovered 80% of its fully recovered value.

FIG. 19. The decay of the three-pulse stimulated echo in $KBr_{0.50}(CN)_{0.50}$ at 10 mK as a function of $t = \tau_{13} + \tau_{12}$ for $\tau_{12} = 2$ μs ($\bullet$), $\tau_{12} = 10$ μs ($\times$), and $\tau_{12} = 20$ μs ($\circ$). Solid lines are guides to the eye.

the actual spin-lattice relaxation time. The decay times for the initial part of the stimulated-echo decays for three of the $KBr_{1-x}(CN)_x$ samples are plotted in Fig. 20. The $x=0.50$ decay times are nearly identical to the T_1 values measured with the three-pulse inversion-recovery experiment (Fig. 14), and follow roughly the expected $\tanh(E/2kT)$ dependence. Decay times for the $x=0.03$ and 0.20 samples fall significantly below T_1 values measured with the three-pulse inversion-recovery experiment, but this fact may simply reflect the inaccuracy involved in using stimulated echoes to measure T_1.

Stimulated-echo results from the $x=0.00034$ sample showed anomalously long relaxation times such as those seen in the inversion-recovery experiment. At short times, the stimulated echo at 10 mK decayed with a time of 250 μs, and at long times (10 ms) the decay time was about 36 ms. These values are consistent with the values of 180 μs and 57 ms from the three-pulse inversion-recovery experiment at 10 mK. A second important point is that, as the time τ_{12} between the first two pulses was increased, the decay rate increased dramatically, showing the existence of spectral diffusion at this concentration.

V. DISCUSSION

We have described measurements of four fundamental properties of the tunneling centers in $KBr_{1-x}(CN)_x$: dipole moment p, phonon coupling γ, density of strongly coupled states $\bar{P}$, and dephasing time T_2. We now discuss trends in these properties as a function of cyanide concentration.

First, one notes that the coupling strengths of CN tunneling centers to electric and strain fields do not vary significantly with cyanide concentration. The dipole moment varies by less than a factor of 1.5 throughout the concentration range studied, and γ varies by only a factor of 2, suggesting that the dominant excitations are

similar and independent of x. This result is consistent with a model that attributes the glassy excitations in high-concentration $KBr_{1-x}(CN)_x$ to single cyanide molecules.[47] [One cannot rule out contributions from collective motions of groups of cyanide molecules that, as a group, have nearly the same values of p and γ as single CN tunneling centers. Pairs of impurity dipoles with the same electric-dipole moment as a single impurity ions have been observed[48] in alkali halides doped with OH, and some anomalous dielectric data in $KBr_{1-x}(CN)_x$ have been explained by similar excitations.[49]]

The tunneling density of states, extracted from dielectric constant, echo amplitudes, and short-time specific-heat data (for states with $E \sim 0.1$ K) are shown by the upper curve in Fig. 21. Each set of data has been normalized to its value at $x=0.70$. The dielectric data (solid circles in figure, data are from Table I), from measurements between 0.1 and 1 K, represent those states which have $E \approx 0.2$ to 2 K. The echo amplitudes (squares) are from the maximum value of the excitation curves in Fig. 7, and represent those states with $E \approx 0.04$ K (corresponding to 0.79 GHz). The specific-heat points (triangles) are taken at 0.1 K and 1 ms, representing states with $E \sim 0.2$ K (data from Ref. 12). The smooth curve is a guide to the eye. The agreement between the data sets is quite good. The large value for the $x=0.00034$ dielectric point can be explained by noting that in this sample the density of states peaks near 1.25 K and decreases for smaller energy splittings (Sec. IV A). Since the dielectric point is from data between 0.1 and 1 K, it probably represents the density of states near this peak. The specific heat at 0.1 K and the echo amplitude at 0.79 GHz represent lower-energy states in the tail of this distribution, resulting in a lower apparent $\bar{P}$. For the higher-concentration samples, the density of states is more nearly constant with energy, so this discrepancy should not occur. Specific-heat measurements[12] at lower cyanide concentration than shown in Fig. 21 display a linear increase in density of states
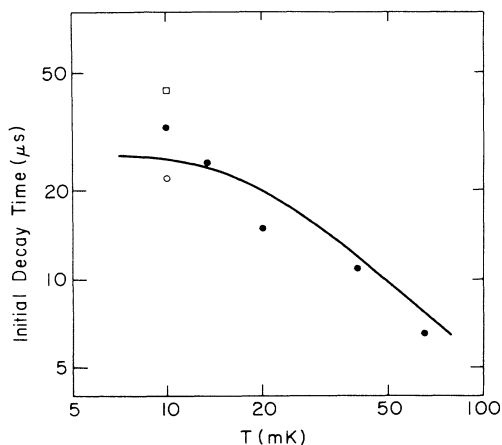

FIG. 20. Initial decay rates from stimulated-echo experiments for $x=0.03$ ($\bigcirc$), $x=0.20$ ($\square$), and $x=0.50$ ($\bullet$). The solid line represents the $\tanh(E/2kT)$ dependence expected for one-phonon processes, and is adjusted in amplitude to fit the $x=0.50$ data.
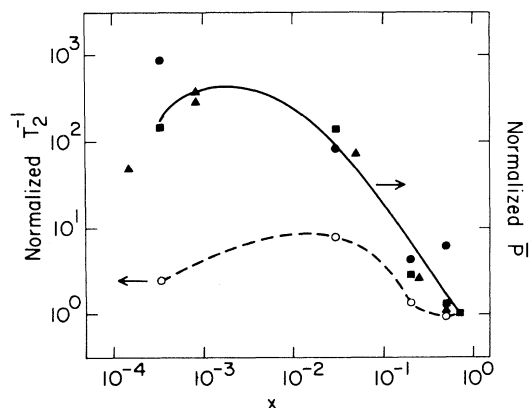

FIG. 21. Upper curve represents the density of states of tunneling centers, $\bar{P}$, from time-dependent specific heat ($\blacktriangle$, Ref. 12), dielectric constant ($\bullet$), and echo amplitudes ($\blacksquare$). The lower curve ($\bigcirc$) is dephasing rates (T_2^{-1}) at 10 mK, from Fig. 10. All sets of data have been normalized to their value at $x=0.70$. The curves are guides to the eye.

with concentration. In the region of $x \approx 0.001\text{--}0.01$, however, a maximum occurs in $\bar{P}$. The subsequent decrease is caused by strong interactions between CN molecules, which tend to spread the distribution of energy splittings over a much broader range, decreasing the density of states at $E \leq 1$ K.

Normalized dephasing rates at 10 mK are also plotted in Fig. 21 (open circles). One might expect that T_2^{-1} should be proportional to $\bar{P}$ [Eq. (7)], since a larger density of states means a larger number of thermally active states to cause dephasing. Figure 21, however, shows that such a proportionality is *not* observed in our experiments. Instead, there is a systematic departure of the $\bar{P}$ and T_2^{-1} curves as the cyanide concentration is decreased from $x=0.70$. At the lowest concentrations the dephasing rate is nearly two orders of magnitude smaller than expected from the large density of states of excitations.

An explanation for the relatively slow dephasing rates seen in the low-concentration $KBr_{1-x}(CN)_x$ samples is that, although there are a large number of quickly relaxing states in these samples (large $\bar{P}$), there is a proportionately reduced number of the slower states compared to the higher-concentration samples. Since the slow states in glasses and in high-concentration $KBr_{1-x}(CN)_x$ are expected to produce a large fraction of the dephasing,[25] a reduction in the fraction of these states would result in lower dephasing states. This scenario is illustrated schematically in Figs. 22(a) and 22(b). Figure 22(a) shows the distribution of relaxation rates of the tunneling model, which is approximately valid for $KBr_{0.5}(CN)_{0.50}$. The density of states $\bar{P}$ of quickly relaxing states can be thought of as roughly the area of the shaded region under the density-of-states curve in the right half of Fig. 22(a). We postulate that as x decreases, the density-of-states curve as a function of relaxation rate becomes more like the curve in Fig. 22(b). This distribution has a large number of quickly relaxing states, but proportionally fewer of the slower states. In this case, a measurement of $\bar{P}$ would observe most of the states. Since there are only a few slow states, however, the dephasing rate would be proportionally smaller at low x, resulting in the divergence of the T_2^{-1} and $\bar{P}$ curves shown in Fig. 21.

Recent measurements[16] of time-dependent specific heat in $KBr_{1-x}(CN)_x$ seem to support this picture. Samples with $0.008 \leq x \leq 0.05$ were measured near 0.1 K for times ranging from 0.3 ms to 10 s. Within this time and temperature window the distribution of relaxation times shifts towards longer times with increasing cyanide concentration.

The slowly relaxing states seen in the specific-heat experiments[16] have been interpreted as small clusters of CN molecules coupled elastically. While this explanation is possible, we believe that the slow states seen in both specific-heat and echo experiments can be more simply explained as asymmetric tunneling centers. We suggest that the distributions of Fig. 22 should be interpreted as an increase in the fraction of asymmetric tunneling centers with increasing x.[50] This variation of tunneling-center symmetry can be explained as a result of changes in the distribution of barriers to CN reorientation. Dielectric loss measurements[31,32,51] above 10 K reveal a
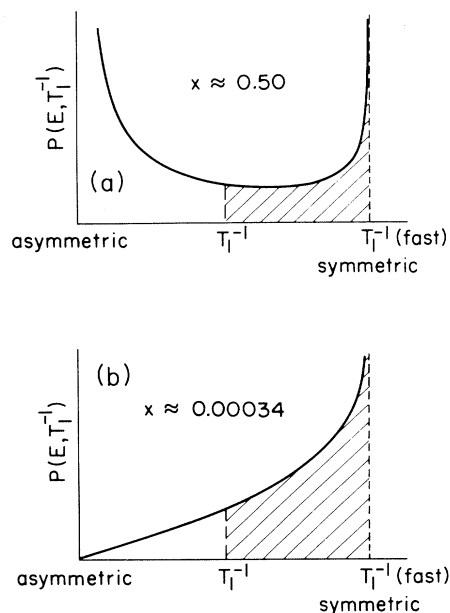

FIG. 22. Postulated variation in the distribution of relaxation rate with cyanide concentration. (a) The relaxation-rate distribution of the tunneling model, which is approximately correct for $KBr_{0.50}(CN)_{0.50}$. (b) Possible distribution of rates for the low-concentration sample.

barrier height which is about 650 K in $KBr_{0.50}(CN)_{0.50}$, and decreases with decreasing concentration. At the lowest concentrations, infrared spectroscopy[8] reveals a 50-K barrier. Since the tunnel splitting Δ_0 of a tunneling center depends on barrier height approximately as $\exp(V^{1/2})$, a decreasing average barrier height corresponds to an increasing average value of Δ_0. The distribution in Δ, on the other hand, should be flat regardless of x for those states of interest in experiments below 1 K, since this distribution is expected to be centered at zero with a width $\gg 1$ K. Combining a constant distribution in Δ with a distribution in Δ_0 that shifts towards higher values with decreasing x, one finds a trend towards the more symmetric (larger Δ_0), quickly relaxing states at lower x. We believe, therefore, that the dielectric loss experiments at higher temperature are consistent with our conclusions regarding the symmetry of tunneling centers below 1 K.

The $x=0.03$, 0.20, and 0.50 dielectric data of Fig. 5 might appear to be inconsistent with this picture since these data show an increasingly strong relaxational term in $\Delta\epsilon/\epsilon$ with decreasing x. We suggest, however, that a large part of the positive $d\epsilon/dT$ above 1 K for these samples is not due to the tunneling relaxation of asymmetric tunneling centers, but rather is thermally activated reorientation. From Fig. 4, it is apparent that the freezing of thermally activated CN reorientations decreases in temperature with decreasing x and begins to infringe on the temperature regime shown in Fig. 5, so probably much of the rapid increase in ϵ above 1 K is due to such thermally activated processes.

A different conclusion regarding the dependence of the

symmetry distribution on x was reached in a study[17] of acoustic properties of $KBr_{1-x}(CN)_x$ at low temperature. Variations of sound velocity and acoustic absorption were measured for $x=0.25$ and 0.50 $KBr_{1-x}(CN)_x$ samples in the temperature range 0.1–8 K. Fitting the data to a modified tunneling model with adjustable distributions, it was concluded that the distribution of tunneling centers in the $x=0.25$ sample was weighted towards the slowly relaxing states in comparison to the distribution observed in the $x=0.50$ sample—a direct contrast to our conclusion. In response, we first note that the acoustic study covered a fairly small concentration range in comparison to the present dielectric study. In addition, we point out that the conclusion of the acoustic study resulted from the observation of a large amount of relaxation in the $x=0.25$ sample above 1 K. This relaxation was attributed to the tunneling of very asymmetric tunneling centers. We believe, however, that a large part of the relaxation observed was not due to tunneling effects, but rather was thermally activated relaxation. In our dielectric constant measurements an excess relaxation term was also observed above 1 K in the $x=0.03$ and 0.20 samples (Fig. 5). However, this relaxation was attributed to the tail of the thermally activated freezing seen in Fig. 4. In brief, we believe that the conclusions of the acoustic study result from a differing interpretation of the character of relaxation above 1 K.

In conclusion, dielectric constant as well as dielectric-echo experiments have probed the tunneling excitations in $KBr_{1-x}(CN)_x$ over a broad cyanide concentration range. It was found that the coupling strength of the tunneling centers to electric and elastic fields does not change significantly with cyanide concentration, although a distribution in p was seen for $x \geq 0.20$. The distribution in relaxation times, however, appears to vary greatly among samples, as evidenced by a comparison of T_2^{-1} and $\bar{P}$ versus x. We interpret this result in terms of the tunneling model for glasses, where for low x the fraction of asymmetric states is decreased greatly relative to its value in $KBr_{0.50}(CN)_{0.50}$ or in other glassy solids.

ACKNOWLEDGMENTS

*Present address: Center for Space Microelectronics Technology, Jet Propulsion Laboratory, California Institute of Technology, Pasadena, California 91109.

[1]K. Knorr and A. Loidl, Phys. Rev. B **31**, 5387 (1985).

[2]U. G. Volkmann, R. Bohmer, A. Loidl, K. Knorr, U. T. Höchli, and S. Haussuhl, Phys. Rev. Lett. **56**, 1716 (1986).

[3]K. Knorr, U. G. Volkmann, and A. Loidl, Phys. Rev. Lett. **57**, 2544 (1986).

[4]J. F. Berret, P. Doussineau, A. Levelut, and W. Schön, Z. Phys. B **70**, 485 (1988).

[5]F. Lüty, Phys. Rev. B **10**, 3677 (1974).

[6]Hans U. Beyeler, Phys. Rev. B **11**, 3078 (1975).

[7]M. Gomez, S. P. Bowen, and J. A. Krumhansl, Phys. Rev. **153**, 1009 (1967).

[8]A. L. Verma, J. Phys. C **13**, 2009 (1980).

[9]P. P. Peressini, Ph.D. thesis, Cornell University, 1973 and Cornell Materials Science Center Report No. 2065, 1973 (unpublished).

[10]J. N. Dobbs, M. C. Foote, and A. C. Anderson, Phys. Rev. B **33**, 4178 (1986).

[11]W. D. Seward and V. Narayanamurti, Phys. Rev. **148**, 463 (1966).

[12]J. J. De Yoreo, W. Knaak, M. Meissner, and R. O. Pohl, Phys. Rev. B **34**, 8828 (1986).

[13]D. Moy, J. N. Dobbs, and A. C. Anderson, Phys. Rev. B **29**, 2160 (1984).

[14]*Amorphous Solids, Low-Temperature Properties,* edited by W. A. Phillips (Springer-Verlag, Berlin, 1981).

[15]M. T. Loponen, R. C. Dynes, V. Narayanamurti, and J. P. Garno, Phys. Rev. Lett. **45**, 457 (1980); M. Meissner and K. Spitzman, *ibid.* **46**, 265 (1981).

[16]W. Knaak and M. Meissner, in *Disordered Systems and New Materials,* Proceedings of the International School of Con-

densed Matter Physics, edited by A. M. Prohorov and M. Borissov (World Scientific, Singapore, 1988).

[17]J. F. Berret, P. Doussineau, A. Levelut, M. Meissner, and W. Schön, Phys. Rev. Lett. **55**, 2013 (1985).

[18]P. W. Anderson, B. I. Halperin, and C. M. Varma, Philos. Mag. **25**, 1 (1972).

[19]W. A. Phillips, J. Low Temp. Phys. **7**, 351 (1972).

[20]M. v. Schickfus and S. Hunklinger, J. Phys. C **9**, L439 (1976).

[21]B. Golding and J. E. Graebner, Phys. Rev. Lett. **37**, 852 (1976).

[22]B. Golding, M. v. Schickfus, S. Hunklinger, and K. Dransfeld, Phys. Rev. Lett. **43**, 1817 (1979).

[23]L. Bernard, L. Piché, G. Schumacher, J. Joffrin, and J. Graebner, J. Phys. (Paris) Lett. **39**, L126 (1978).

[24]W. B. Mims, in *Electron Paramagnetic Resonance,* edited by S. Geschwind (Plenum, New York, 1972), p. 263.

[25]J. L. Black and B. I. Halperin, Phys. Rev. B **16**, 2879 (1977).

[26]D. Moy, Ph.D. thesis, University of Illinois, Urbana, 1983.

[27]J. M. Rowe, J. J. Rush, S. M. Shapiro, D. G. Hinks, and S. Susman, Phys. Rev. B **21**, 4863 (1980).

[28]D. L. Fox, B. Golding, and W. H. Haemmerle, Phys. Rev. Lett. **49**, 1356 (1982).

[29]B. Golding, D. L. Fox, and W. H. Haemmerle, Physica **109&110B**, 2039 (1982).

[30]M. C. Foote, Ph.D. thesis, University of Illinois, Urbana, 1988.

[31]F. Lüty, in *Defects in Insulating Solids,* edited by V. M. Tuchevich and K. K. Shvarts (Springer-Verlag, Berlin, 1981).

[32]N. O. Birge, Y. H. Jeong, Sidney R. Nagel, S. Bhattacharya, and S. Susman, Phys. Rev. B **30**, 2306 (1984).

[33]R. P. Lowndes and D. H. Martin, Proc. R. Soc. London Ser. A **316**, 351 (1970).

[34]H. S. Sack and M. C. Moriarty, Solid State Commun. **3**, 93

(1965); V. Narayanamurti and R. O. Pohl, Rev. Mod. Phys. **42**, 201 (1970).

[35]J. F. Berret and M. Meissner, in *Phonon Scattering in Condensed Matter V*, edited by A. C. Anderson and J. P. Wolfe, Springer Series in Solid-State Sciences Vol. 68 (Springer-Verlag, Berlin, 1986).

[36]W. A. Phillips, Philos. Mag. B **43**, 747 (1981).

[37]M. v. Schickfus and U. Strom, Phys. Rev. B **28**, 1068 (1983).

[38]G. Baier, M. v. Schickfus, and C. Enss, Europhys. Lett. **8**, 487 (1989).

[39]D. L. Huber, M. M. Broer, and B. Golding, Phys. Rev. Lett. **52**, 2281 (1984).

[40]B. Golding (unpublished).

[41]J. Hegarty, M. M. Broer, B. Golding, J. R. Simpson, and J. B. MacChesney, Phys. Rev. Lett. **51**, 2033 (1983).

[42]B. Golding, J. E. Graebner, and W. H. Haemmerle, Phys. Rev. Lett. **44**, 899 (1980).

[43]W. A. Phillips, Proc. R. Soc. London Ser. A **319**, 565 (1970).

[44]J. E. Graebner and B. Golding, Phys. Rev. B **19**, 964 (1979).

[45]Reference 25 does predict a two-pulse echo decay in glasses with a decay constant that varies as T^2, as was seen in SiO_2 glass. This theory only applies, however, to the short-time limit, where the decay is predicted to be Gaussian. Since Gaussian decays have not been observed in glasses, it is believed that this short-time regime is inappropriate to describe the echo experiments in glasses. See also P. Hu and L. R. Walker, Solid State Commun. **24**, 813 (1977); R. Maynard, R. Rammal, and R. Suchail, J. Phys. (Paris) Lett. **41**, L291 (1980).

[46]W. J. Brya and P. E. Wagner, Phys. Rev. **157**, 400 (1967).

[47]A theory based on this idea is presented in M. Meissner, W. Knaak, James P. Sethna, Kenneth S. Chow, J. J. De Yoreo, and R. O. Pohl, Phys. Rev. B **32**, 6091 (1985); James P. Sethna and Kenneth S. Chow, Phase Transitions **5**, 317 (1985).

[48]R. C. Potter and A. C. Anderson, Phys. Rev. B **24**, 4826 (1981).

[49]G. Baier, C. Enss, and M. v. Schickfus, Phys. Rev. B **40**, 9868 (1989).

[50]One might argue that the double-well picture is invalid at low x because an isolated CN ion is affected by an eightfold potential. We point out, however, that the echo experiments observe only states with $E \simeq 40$ mK. Such states are sufficiently distorted from the isolated CN configuration that most likely only two potential minima are accessible.

[51]Richard M. Ernst, Lei Wu, Sidney R. Nagel, and Sherman Susman, Phys. Rev. B **38**, 6246 (1988).